Mendeleev Communications

Mendeleev Commun., 2025, **35**, 484–486

Ordered and disordered zirconia-modified silica supports in diclofenac hydrodechlorination over palladium catalyst

Ekaterina S. Lokteva,*[a] Evelina G. Khachatryan,[a] Mikhail D. Pesotskiy,[a] Elena V. Golubina,[a] Konstantin I. Maslakov,[a] Igor Yu. Kaplin,[a] Sergey I. Kirikov[b] and Sergey V. Maksimov[a]

[a] *Department of Chemistry, M. V. Lomonosov Moscow State University, 119991 Moscow, Russian Federation. Fax: +7 495 939 4575; e-mail: LES@kge.msu.ru*

[b] *Institute of Chemistry and Chemical Technology, Siberian Branch of the Russian Academy of Sciences, 660036 Krasnoyarsk, Russian Federation*

DOI: 10.71267/mencom.7717

The performance of Pd catalysts supported on ordered (ZrSBA) or disordered (ZS) ZrO_2-modified SiO_2 was evaluated in the hydrodechlorination of ecotoxic diclofenac with H_2 in an aqueous medium at 30 °C, after pre-reduction of the catalysts with H_2 at 320 °C or in water at 30 °C. The ordered 0.1 wt% Pd/ZrSBA catalysts with lower Pd content, reduced at both temperatures, showed similar diclofenac conversion rates that were comparable to or much higher than those of the 0.86 wt% Pd/ZS catalysts reduced at 320 or 30 °C, respectively. A comprehensive analysis using XRD, N_2 adsorption, TEM-EDA, TPR and XPS techniques revealed the presence of larger Pd nanoparticles, a reduced degree of Pd decoration with silica and slightly improved reducibility of Pd/ZrSBA at 30 °C compared to Pd/ZS, which resulted in a superior efficiency of the former catalyst.

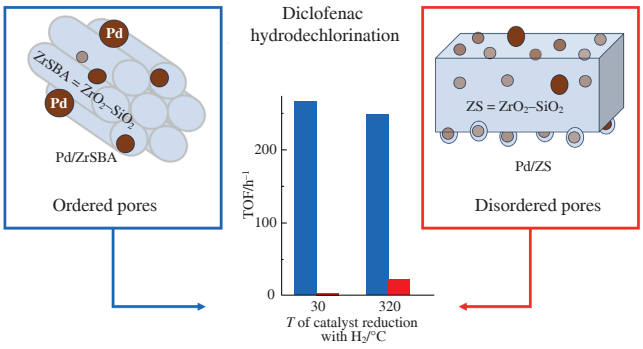

Keywords: diclofenac, hydrodechlorination, catalyst, mesopores, ordered structure, catalyst reduction.

Hydrodechlorination[1–3] is a very efficient method for water purification from chlorinated environmental pollutants such as the non-steroidal anti-inflammatory drug diclofenac. It can be converted to much less toxic 2-(2-anilinophenyl)acetate (APA).[1] Hydrodechlorination is considered a structure-sensitive reaction[2] in which the catalytic activity depends on the Pd particle size, but the nature of the dependence remains controversial. There are reports that the efficiency is higher for both smaller and larger nanoparticles.[4] Partially oxidized palladium ($Pd^{\delta+}$), which can activate the C–Cl bond, favors high hydrodechlorination activity of the catalyst.[5] This effect is characteristic of electron-deficient small nanoparticles that donate electron density to the support. Large Pd particles are prone to hydride formation and are more stable toward HCl, a by-product of hydrodechlorination.[6] The use of an ordered support can help to tune the Pd particle size.

It has been previously shown that Pd^{2+} supported on Al_2O_3, ZrO_2 and disordered mesoporous ZrO_2–SiO_2 (hereinafter referred to as ZS) can be reduced to some extent with H_2 even under very mild conditions (30 °C, aqueous suspension), *i.e.*, in fact, under hydrodechlorination conditions.[7,8] The low-temperature treatment prevents sintering of small palladium particles, which is more likely to occur during reduction at high temperature. The ability of the supported PdO particles to undergo mild reduction depends on the nature and textural properties of the support. X-ray photoelectron spectroscopy (XPS) revealed Pd migration from the surface into the bulk of Al_2O_3 and ZS supports during reduction at 320 °C.[9] The ordered mesoporous supports can prevent Pd depletion of the catalyst surface during preparation.

In this work, zirconia-modified ordered mesoporous silica SBA-15 with Si/Zr = 92 : 8 (ZrSBA) and disordered mesoporous ZrO_2–SiO_2 with Si/Zr = 55 : 45 (ZS) were used as supports for palladium catalysts 0.1 wt% Pd/ZrSBA and 0.86 wt% Pd/ZS, which after reduction under mild (30 °C) and severe (320 °C) conditions were tested in the hydrodechlorination of diclofenac and characterized by a series of physical methods. Details of the preparation, catalytic testing and analytical methods are provided in Online Supplementary Materials.

The specific surface area, pore diameter and pore volume of the ZrSBA support calculated from the low-temperature N_2 sorption isotherms are higher than those of ZS (Table S1, see Online Supplementary Materials), mainly due to the ordered pore structure of ZrSBA and the narrower pore size distribution (data not shown). Furthermore, different Pd and Zr loadings may also affect these parameters.

The ordered mesopore structure in ZrSBA was confirmed by small-angle X-ray diffraction (XRD): the diffraction pattern [Figure 1(*a*)] shows a typical distinct peak at 2θ 0.9° and a series of low-intensity peaks in the range of 1.2–2°. The XRD patterns [Figure 1(*b*)] of the Pd/ZrSBA and Pd/ZS catalysts reduced at 30 °C show a broad halo with a maximum at 20–25° corresponding to amorphous SiO_2 and a low-intensity reflection of Pd^0 at about 40° (ICDD card 46–1043). The low intensity of this peak confirms the low Pd content, while the large peak width suggests a high dispersion of palladium in both samples. No reflections of

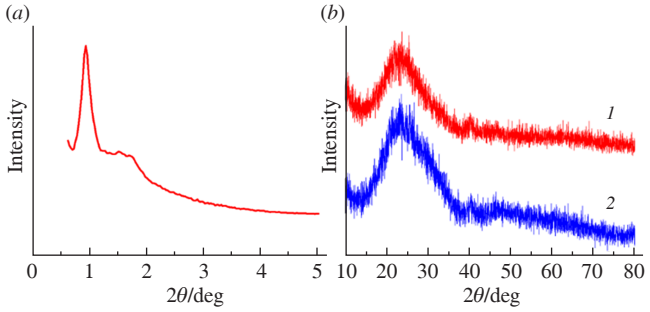

Figure 1 (*a*) Small-angle XRD pattern of ZrSBA and (*b*) XRD patterns of (*1*) Pd/ZrSBA(30) and (2) Pd/ZS(30).

crystalline ZrO_2 were detected, indicating the absence of large zirconia crystallites.

The TEM-EDA data (Figure S1, see Online Supplementary Materials) also confirm the ordered mesoporous structure of ZrSBA in the Pd/ZrSBA(320) catalyst and the uniform distribution of Zr in SiO_2 [Figure S1(*c*)], typical of SBA with a Zr content below 20 at%,[10] which is consistent with the absence of ZrO_2 reflections in the XRD pattern of this catalyst. Identification of Pd particles in TEM images is complicated by the close atomic masses of Zr (91) and Pd (106) and the low Pd/Zr atomic ratio. However, Figure S1(*a*)–(*c*) show that Pd is distributed over some areas of the ZrSBA support, with the sample containing small Pd particles (up to 10 nm), their aggregates and larger particles (from 10 to 80 nm). Some palladium particles are located in the pores of the support, they are indicated by arrows in Figure S1(*a*) and are visible as dark dots in Figure S1(*d*). Comparison of the TEM image arrays shows that the dispersion of Pd in Pd/ZS is significantly higher, since no Pd-containing particles larger than 5 nm were found.

The Pd^0/Pd^{2+} ratios in the unreduced precursors and in the reduced catalysts were calculated from the high-resolution Pd 3*d* XPS spectra. Only Pd^{2+} is present on the surface of the unreduced Pd/ZS precursor (Table 1). The catalyst precursors were calcined in air at 500 °C, so PdO should be the major form of Pd before reduction. Treatment of Pd/ZS with H_2 at 320 °C resulted in complete reduction of surface PdO, whereas only partial reduction (93%) was observed at 30 °C (see Table 1). In contrast, the Pd/ZrSBA precursor contains 32% Pd^0 on the surface even before H_2 treatment. For this catalyst, mild reduction is slightly more efficient than reduction at 320 °C. Notably, Pd^0 was the predominant species on the surface of all reduced catalysts. The Pd/Si and Pd/Zr ratios in the catalysts calculated from the AAS data were compared with the surface ratios after reduction under mild and severe conditions calculated from the XPS data (see Table 1). For unreduced Pd/ZS and Pd/ZS(320), the surface Pd/Si ratio was significantly lower than that calculated for the bulk, suggesting that Pd is located in the subsurface layer. In the case of Pd/ZS(30), the value is higher than that calculated for the bulk, which may be caused by the redistribution of Pd and support components in the aqueous medium. Conversely, the surface Pd/Si ratio for Pd/ZrSBA is much higher than that for the bulk, irrespective of the reduction conditions. Considering the much lower Pd loading in this sample, it is likely to be located mainly near the surface rather than penetrating into the pore walls. The Pd/Si is almost independent of the type and conditions of reduction, making this support more stable in an aqueous medium.

Table 1 XPS data on the surface composition of the catalysts before and after reduction with H_2 in comparison with AAS data for the bulk.

Catalyst	Pd^0	Pd^{2+}	Pd/Si (×10^{-4})		Pd/Zr (×10^{-3})	
			AAS[a]	XPS[b]	AAS[a]	XPS[b]
Pd/ZS	0	100	132	18	16	21
Pd/ZS(30)	93	7		175		37
Pd/ZS(320)	96	4		20		23
Pd/ZrSBA	31	69	7	1000	8	6
Pd/ZrSBA(30)	96	4		1250		7
Pd/ZrSBA(320)	89	11		1000		6

[a]Bulk composition calculated from AAS data. [b]Surface composition calculated from XPS data.

The calculations of the Pd/Zr ratio are not entirely accurate due to the low Pd content in both samples, the low Zr content in Pd/ZrSBA and the overlap of the Pd 3*d* and Zr 3*p* peaks in the XPS spectra. Therefore, it is reasonable to disregard the small discrepancies observed in the Pd/Zr surface-to-volume ratio of both samples. In the case of Pd/ZS, the ratio is slightly higher, while for Pd/ZrSBA it is similar to the bulk concentration and slightly dependent on the reduction conditions of the samples.

The XRD, TEM, nitrogen physisorption and XPS results together indicate that the ordered mesoporous structure of the ZrSBA support is able to localize Pd on the catalyst surface. The Pd/ZrSBA catalyst contains both small Pd nanoparticles inside the pores and larger nanoparticles and aggregates, which are absent in the Pd/ZS sample. This suggests that the particle size distribution is significantly broader in the Pd/ZrSBA catalyst. A clear difference in the reducibility of PdO is expected, which was confirmed by temperature-programmed reduction (TPR) with H_2 (Figure 2). The TPR profiles of both samples show a peak at 65–67 °C corresponding to the decomposition of PdH_x, *i.e.*, when the reactor is filled with H_2/Ar mixture, PdO is reduced to Pd^0, which further absorbs H_2 to form PdH_x. However, the intensity of this peak is higher for Pd/ZrSBA with lower Pd content than for Pd/ZS with higher Pd content. Note that a significant amount of Pd^0 was found by XPS on the surface of unreduced Pd/ZrSBA. The amount of H_2 required to reduce all the PdO contained in the weighed portion of Pd/ZS is consistent with the amount of H_2 released upon decomposition of PdH_x (Table S2). Significantly more H_2 was released from Pd/ZrSBA, possibly due to the presence of relatively large Pd^0 particles detected by TEM, capable of superstoichiometric H_2 uptake. Both TPR profiles show a baseline shift near the negative peak, which can be explained by a superposition of H_2 release upon decomposition of PdH_x and H_2 uptake upon reduction of PdO. In contrast to the ZS support, the TPR profile of Pd/ZS shows additional low-intensity high-temperature peaks at 255 and 359 °C. These may be due to the reduction of a portion of the PdO in the bulk of this sample, which is more strongly bound to the

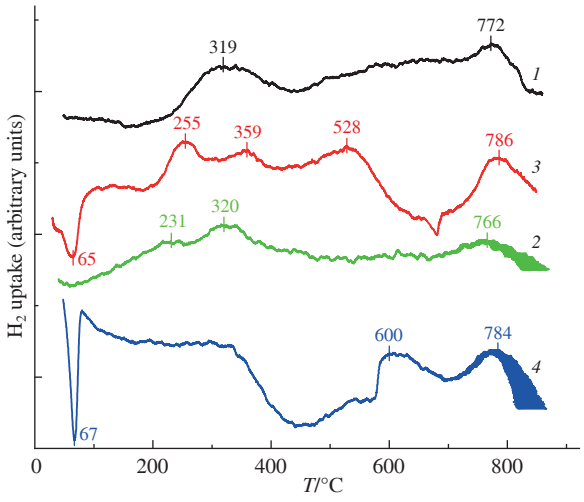

Figure 2 TPR profiles of (*1*) ZS and (*2*) ZrSBA supports, as well as (*3*) Pd/ZS and (*4*) Pd/ZrSBA catalysts.

support, or to the reduction of functional groups on the support surface. No peaks of PdO reduction are observed in the Pd/ZrSBA profile at temperatures up to 350 °C. The easier reducibility of PdO in Pd/ZrSBA can be explained by its preferential location on the outer surface of the support particles.

Hydrodechlorination of diclofenac produced 2-[2-(2-chloroanilino)phenyl]acetate (ClAPA) and APA with a small admixture of products with shorter retention times. The ClAPA content did not exceed 15%, and at high conversions APA was the only product. Figure 3 shows the diclofenac conversion as a function of reaction time for the catalysts reduced at 30 or 320 °C. Figure S1 shows the TOFs calculated as described in Online Supplementary Materials. The results of the catalytic tests can be summarized as follows. (1) The Pd/ZrSBA catalyst is slightly more efficient after reduction at 30 °C than at 320 °C, possibly due to the increased Pd^0/Pd^{2+} ratio and higher Pd concentration on the surface of Pd/ZrSBA(30) compared to Pd/ZrSBA(320), as measured by XPS. (2) The Pd/ZS catalyst is significantly less efficient after mild reduction than after H_2 treatment at 320 °C. According to the XPS data, mild reduction results in a slightly lower Pd^0/Pd^{2+} ratio, but the surface is enriched with Pd. High dispersion of Pd in Pd/ZS before and after reduction at 30 °C results in low PdH_x content, but treatment with H_2 at 320 °C may cause sintering of Pd particles and facilitate the formation of PdH_x under the catalytic reaction conditions. (3) At much lower Pd loading, the Pd/ZrSBA catalyst provided higher diclofenac conversion rate than Pd/ZS after high-temperature reduction and especially after mild reduction due to the location of Pd in the surface layers and its higher accessibility for reactant adsorption. However, this cannot be the only reason, since in the least active catalyst Pd/ZS(30) palladium is also mainly located on the surface. Therefore, the presence of large Pd nanoparticles together with small ones is also important for the catalytic efficiency. The formation of PdH_2 from large Pd particles can provide activated hydrogen for the hydrodechlorination of diclofenac. As a result, the TOF value of 268 h^{-1} for Pd/ZrSBA(30) is significantly higher than the TOF value of 0.04 h^{-1} for Pd/ZS(30) (see Figure S1), although the TOF values are similar after reduction at 320 °C. (4) A significant decrease of the reaction rate after reaching 90% conversion for both catalysts can be explained by the loss of catalyst during sampling for analysis, catalyst deactivation under the action of evolving HCl, as well as adsorption of diclofenac from the solution and its gradual release into the aqueous phase during long-term tests.[11]

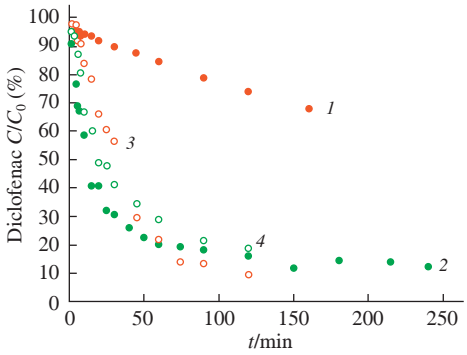

Figure 3 Hydrodechlorination of diclofenac (150 mg dm^{-3}) in an aqueous solution (15 ml) at 30 °C with hydrogen (0.6 dm^3 h^{-1}) over (*1*), (*3*) Pd/ZS and (*2*), (*4*) Pd/ZrSBA catalysts (0.05 g), reduced at (*1*), (*2*) 30 and (*3*), (*4*) 320 °C.

The higher efficiency of the Pd/ZrSBA catalyst may be associated with its ordered mesoporous structure, which prevents Pd migration from the surface into the bulk and improves the accessibility of Pd for reagent adsorption. For the Pd/ZS(30) sample such enrichment is significantly lower, and the Zr/Si ratio is too high (Table S3). The high catalytic efficiency of Pd/ZS(320) compared to Pd/ZS(30) may be due to the coarsening of Pd particles during the high-temperature reduction. Large Pd particles readily form hydride, which has an enhanced ability to activate H_2, in contrast to electron-deficient small Pd nanoparticles.[12] Thus, our work demonstrates the increased efficiency of larger Pd nanoparticles.

This work was carried out within the framework of the State Assignment no. AAAA-A21-121011990019-4 and supported by the M. V. Lomonosov Moscow State University Program of Development.

Online Supplementary Materials

Supplementary data associated with this article can be found in the online version at doi: 10.71267/mencom.7717.

References

1 L. Lonappan, S. K. Brar, R. K. Das, M. Verma and R. Y. Surampalli, *Environ. Int.*, 2016, **96**, 127; https://doi.org/10.1016/j.envint.2016.09.014.
2 J. Xiong, Y. Ma, W. Yang and L. Zhong, *J. Hazard. Mater.*, 2018, **355**, 89; https://doi.org/10.1016/j.jhazmat.2018.05.018.
3 E. G. Dzhabarov, N. N. Petrukhina and E. M. Zakharyan, *Mendeleev Commun.*, 2023, **33**, 839; https://doi.org/10.1016/j.mencom.2023.10.033.
4 B. Coq, G. Ferrat and F. Figueras, *J. Catal.*, 1986, **101**, 434; https://doi.org/10.1016/0021-9517(86)90271-X.
5 N. S. Babu, N. Lingaiah, N. Pasha, J. V. Kumar and P. S. S. Prasad, *Catal. Today*, 2009, **141**, 120; https://doi.org/10.1016/j.cattod.2008.03.018.
6 B. Zawadzki, E. Kowalewski, M. Asztemborska, K. Matus, S. Casale, S. Dzwigaj and A. Śrębowata, *Catal. Commun.*, 2020, **145**, 106113; https://doi.org/10.1016/j.catcom.2020.106113.
7 V. V. Shishova, E. S. Lokteva, G. S. Maksimov, K. I. Maslakov, I. Yu. Kaplin, S. V. Maksimov and E. V. Golubina, *Moscow Univ. Chem. Bull.*, 2024, **79**, 156; https://doi.org/10.3103/S0027131424700123.
8 E. S. Lokteva, M. D. Pesotskiy, E. V. Golubina, K. I. Maslakov, A. N. Kharlanov, V. V. Shishova, I. Yu. Kaplin and S. V. Maksimov, *Kinet. Catal.*, 2024, **65**, 133; https://doi.org/10.1134/S0023158423601183.
9 E. S. Lokteva, V. V. Shishova, K. I. Maslakov, E. V. Golubina, A. N. Kharlanov, I. A. Rodin, M. F. Vokuev, D. S. Filimonov and N. N. Tolkachev, *Appl. Surf. Sci.*, 2023, **613**, 156022; https://doi.org/10.1016/j.apsusc.2022.156022.
10 T. Qiang, J. Zhao and J. Li, *Microporous Mesoporous Mater.*, 2018, **257**, 162; https://doi.org/10.1016/j.micromeso.2017.08.041.
11 O. V. Kharissova, V. A. Zhinzhilo, M. A. Chernomorova, I. E. Uflyand and B. I. Kharisov, *Mendeleev Commun.*, 2023, **33**, 428; https://doi.org/10.1016/j.mencom.2023.04.041.
12 M. Boudart and H. S. Hwang, *J. Catal.*, 1975, **39**, 44; https://doi.org/10.1016/0021-9517(75)90280-8.

Received: 27th December 2024; Com. 24/7717